J. Hydrol. Hydromech., 66, 2018, 1, 32–42
DOI: 10.1515/johh-2017-0041

An unusual kind of diurnal streamflow variation

Jaime G. Cuevas[1, 2, 3*], José L. Arumí[4], Alejandra Zúñiga-Feest[3, 5], Christian Little[6, 7]

[1] Centro de Estudios Avanzados en Zonas Áridas (CEAZA), Av. Raúl Bitrán 1305, La Serena, Chile.
[2] Instituto de Ingeniería Agraria y Suelos, Universidad Austral de Chile, Valdivia, Chile.
[3] Centro de Investigaciones en Suelos Volcánicos (CISVo), Universidad Austral de Chile, Valdivia, Chile.
[4] Facultad de Ingeniería Agrícola, Departamento de Recursos Hídricos, Centro CRHIAM, Universidad de Concepción, Chillán, Chile.
[5] Laboratorio de Biología Vegetal, Instituto de Ciencias Ambientales y Evolutivas, Facultad de Ciencias, Universidad Austral de Chile, Valdivia, Chile.
[6] Instituto Forestal (INFOR), Sede Los Ríos, Fundo Teja Norte s/n, Valdivia, Chile.
[7] Center For Climate and Resilience Research (CR)[2], Chile.
[*] Corresponding author. Tel.: +56 51 2204378. E-mail: jxcuevas@ceaza.cl.

Abstract: During hydrological research in a Chilean swamp forest, we noted a pattern of higher streamflows close to midday and lower ones close to midnight, the opposite of an evapotranspiration (Et)-driven cycle. We analyzed this diurnal streamflow signal (DSS), which appeared mid-spring (in the growing season). The end of this DSS coincided with a sustained rain event in autumn, which deeply affected stream and meteorological variables. A survey along the stream revealed that the DSS maximum and minimum values appeared 6 and 4 hours earlier, respectively, at headwaters located in the mountain forests/ plantations than at the control point in the swamp forest. Et in the swamp forest was higher in the morning and in the late afternoon, but this process could not influence the groundwater stage. Trees in the mountain headwaters reached their maximum Ets in the early morning and/or close to midday. Our results suggest that the DSS is a wave that moves from forests high in the mountains towards lowland areas, where Et is decoupled from the DSS. This signal delay seems to convert the link between streamflow and Et in an apparent, but spurious positive relationship. It also highlights the role of landscape heterogeneity in shaping hydrological processes.

Keywords: Evapotranspiration; Groundwater; Riparian zones; Streamflow; Swamp forests.

INTRODUCTION

The pattern of higher streamflow at dawn and lower streamflow during the afternoon has been identified for the past 80 years (Gribovszki et al., 2010). According to Graham et al. (2013), the source of these signals and the way in which they are propagated to stream gauging sites are poorly understood. The traditional concept establishes that groundwater is the link between the plant cover and the stream (Gribovszki et al., 2008; Szilágyi et al., 2008). When the groundwater level decreases at times of high evapotranspiration (Et), this decreases the stream recharge (Hughes, 2010), which lowers its stage. Conversely, when Et is low, water can be replenished in sites with depressed levels (including the stream) from groundwater coming from the uplands, from areas where phreatic water was not affected by an Et cycle (grasslands for example). However, other evidence suggests that the link might also be mediated by water found in the vadose zone (Bond et al., 2002; Bren, 1997; Burt, 1979; Graham et al., 2013). For example, Barnard et al. (2010), Moore et al. (2011) and Puchi (2013) found correlations between soil moisture, streamflow and evapotranspiration. Conversely, Brooks et al. (2010), based on a study with stable isotopes, demonstrated that water used by trees and that which feeds streams have different origins, where the latter is "mobile water", and the former is more tied to the soil. At present, it is not completely clear whether vadose zone moisture is a cause of diurnal streamflow variations or a correlate of groundwater fluctuations. Therefore, more research is necessary in this regard.

In spite of the fact that diurnal streamflow fluctuations have been studied for a long time, this topic has been comparatively little analyzed with respect to other hydrological characteristics. However, it has received renewed interest in recent years (Carlson Mazur et al., 2014; Graham et al., 2013; Mutzner et al., 2015). Some studies have even tested the possibility of artifacts caused by modern pressure transducers (Cuevas et al., 2010; Gribovszki et al., 2013; McLaughlin and Cohen, 2011). Even though some instruments can overestimate diurnal fluctuations, the consensus is that they are real.

Over the course of our hydrological research in a swamp forest in southern Chile, we noted an unusual pattern expressed as a higher streamflow close to midday, while the lowest streamflow was detected close to midnight. This is exactly the opposite pattern of an evapotranspiration-driven cycle. The studied catchment was not affected by snow melting or by soil freezing and thawing (Caine, 1992; Jordon, 1983), nor by water diversion for human use, nor does it experience heavy afternoon rains as occur in the tropics (Wain, 1994), which could all be evident explanations for the phenomenon. Long time lags, such as those found in this study, have scarcely been reported in the literature (Wondzell et al., 2007). When they have been detected, they have been explained in the context of water signals travelling through the catchments. Thus, the present finding motivated a detailed analysis of the variation. Therefore, this study's objective was to provide an explanation for this peculiar pattern, which challenges our present knowledge on the topic. Possible drivers were investigated, namely stream variables, groundwater, biological factors, meteorology, geomorphology, and land cover.

MATERIALS AND METHODS

Study site

The work was conducted at the Austral Experimental Livestock and Agriculture Station, located in the Los Ríos Region in southern Chile (39° 46' 55" S, 73° 13' 24" W), 4 km north of the city of Valdivia, and 15 km from the Pacific Ocean (Fig. 1a).

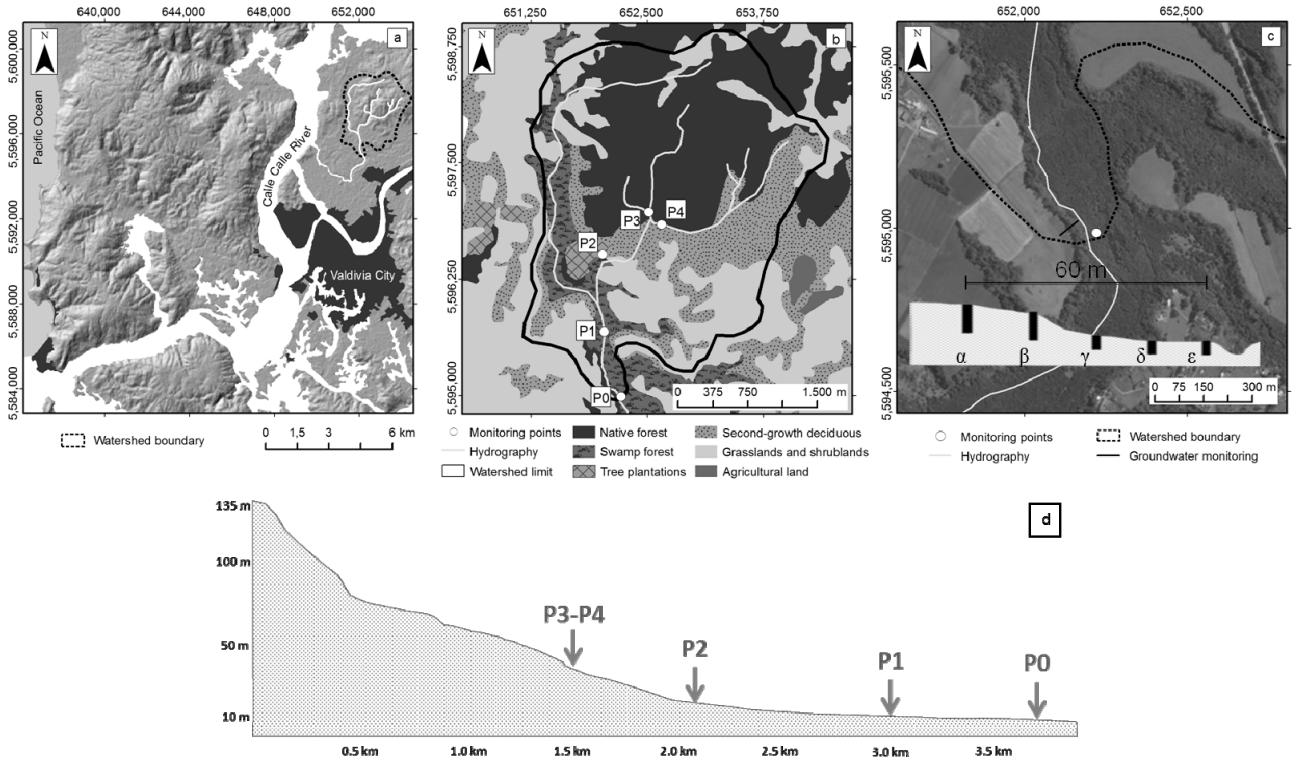

Fig. 1. a) Location of the study site in southern Chile. b) Delimitation of the Santa Rosa watershed. c) Detail of the main studied site (P0), showing the transect for groundwater evaluation (black line), and the position of boreholes along the slope. d) Longitudinal profile of the studied stream, with the monitoring points for stream stage (P0 to P4). Evapotranspiration rates were monitored for the trees *Blepharocalyx cruckshanksii* (at the site P1), *Eucalyptus nitens* and *Nothofagus dombeyi* (both at the site P3).

The climate is humid temperate (Amigo and Ramírez, 1998), with an average annual temperature of 12°C. Annual rainfall is 2,500 mm; most of the rain is concentrated in the winter season (June – August).

We studied the Santa Rosa watershed, whose creek is 5–6 m wide with a discharge of 45–1,107 L s^{-1} (in the summer and winter, respectively). The creek forms part of a watershed whose approximate area is 9.29 km^2 (Fig. 1b), flowing through the middle of a 250 m-wide native forest.

The geomorphology is mainly composed of alluvial terraces, with the uplands (0.5–3° slope) covered by grasslands of *Lolium perenne* L. (perennial ryegrass). A forested slope (25 m wide, 35° inclination) then connects with the floodplain (4° slope), which is also covered by native forest. The grasslands are located about 17 m a.s.l., while the Santa Rosa Creek is located at 4 m a.s.l. The stream begins to rise up to 140 m a.s.l. between 1.8 and 4.3 km upstream of the main studied site (named control point, P0), where second-growth, evergreen native forests and exotic tree plantations are found in the mountain headwaters (Figs. 1b, d).

The forested slope and the foothills below the mountain headwaters are dominated by second-growth deciduous forests of *Nothofagus obliqua* var. *obliqua* trees, *Chusquea quila* bamboo, and *Hedera helix*, an exotic vine. *N. obliqua* corresponds mainly to the indigenous vegetation that dominated the grassland area before its utilization for livestock breeding. The riparian vegetation found in the floodplain is characterized principally by native trees including *Blepharocalyx cruckshanksii*, *Myrceugenia exsucca*, and *Drimys winteri* var. *chilensis*, with few individuals of *N. obliqua*. The second-growth evergreen native forest found in the mountainous headwaters is mainly made up of arboreal individuals of *Aextoxicon punctatum*, *Amomyrtus luma*, *Luma apiculata*, *Lomatia hirsuta*, and *Nothofagus dombeyi*; vines of *Cissus striata* and *Boquila trifoliolata*, and bamboo thickets of *Chusquea quila*. Finally, exotic species include *Eucalyptus* spp., *Pseudotsuga mensiezii* and *Pinus radiata.* With the exception of *N. obliqua*, all of the flora is evergreen. In terms of land cover, grasslands account for 22% of the watershed, swamp forests 16%, exotic tree plantations 0.74%, second-growth evergreen forests 38%, and the second-growth deciduous forests on the foothills and on the slope adjacent to the swamp forests the remaining 23.26% of the area (Fig. 1b).

All of the soils are volcanic, but they belong to different orders. In the alluvial terraces adjacent to the control point, the soil corresponds to an Andisol, Valdivia series (Duric Hapludand or a Petroduri-Silandic Andosol; WRB, 2006). This soil is characterized by a low bulk density (< 0.9 Mg m^{-3}, Dörner et al., 2010) and a well-defined inter- and intra-aggregate pore system (Dörner et al., 2010), which allows for a large porosity and water holding capacity with a high saturated hydraulic conductivity, and thus a high water infiltration rate (Dörner et al., 2009). In the mountain headwaters, on the other hand, the soils belong to the order Acrisol (WRB, 2006) (also termed as Ultisols; Soil Survey Staff, 1999). This soil has a red clay aspect, and the corresponding series is Los Ulmos. Bulk density is 1.0 Mg m^{-3} (CIREN, 2001). In general, Ultisols are less porous than Andisols, and are more prone to overland flow.

General approach

Our study's overall method consisted of: i) documenting the diurnal streamflow signal (DSS) as detected by pressure loggers submerged in the stream. ii) Then, we confirmed whether the pattern was real by visually inspecting the stream during 24 h-cycles. iii) We also examined the full hydrological and rainfall series to detect when the DSS appeared and disappeared. iv) The stream temperature, which is a variable influenced by both

meteorological and hydrological factors, was also seasonally monitored. v) The influence of groundwater from adjacent floodplains was studied as well, since this has been documented in previous studies as a source of water for DSS. vi) We determined the signal timing in order to assess the precise moment when maxima and minima occurred, in addition to their variations throughout the season. vii) A more detailed study was carried out along a transect encompassing a longer extension of the Santa Rosa Creek, to assess the evolution of the DSS on both a temporal and spatial scale. viii) The influence of evapotranspiration was measured in representative trees in order to establish a link between plant Et, ground- and surface water. ix) The analysis of meteorological variables allowed for a longer time record of variables influencing potential Et (Et_0). x) Watershed geomorphology was considered due to the differences between the mountain headwaters and lowland areas' slopes, aspects, and altitudes. xi) Finally, the contribution of different land cover was assessed, since the studied watershed has multiple uses (mainly forestry, livestock and agriculture). Considering all of the aforementioned elements, we proposed an explanation for the observed DSS.

Streamflow variations

A HOBO U20-001-01 pressure logger (Onset Computer Corporation, Bourne, USA) was placed in the middle of the Santa Rosa Stream from May 2014 to November 2015 (the "control point, P0", Figs. 1b, c). This equipment, which measures pressure and temperature, was hung from a steel chain connected to the top cap of a PVC tube. The barometric pressure compensation logger was also placed in the stream, but within a PVC tube that was closed at the bottom to prevent water from entering. The top end of the PVC tube was left open, but was isolated from rain with a non-hermetic plastic "hat". The same barometer was used for the compensation of all the loggers installed in surface and groundwaters (see the following sections), making only some corrections necessary due to differences in altitude between the sampled wells and the stream (12 Pa m^{-1}). The interval of measurement was every 15 min.

The stream gauge was also visually inspected during two 24 h-surveys of water stage, in order to validate the logger's measurements. With this purpose, we installed a stake into the streambed with a tape measure glued to it. This tape was calibrated in millimeters and was carefully inspected from the same point of view, to avoid parallax errors, and using a flashlight at night.

The stream stages were converted into streamflow by using direct measurements with a Seba F1 current meter (Eijkelkamp, The Netherlands) at the studied stream reach P0, 100 m upstream and 100 m downstream; these measurements were then averaged to give a unique value. The stream's velocities were measured at 20 and 80% of the stream depth, in several sections of each of the three studied transects. Discharges were measured 11 times from December 2012 to August 2015 and were related to water stage by means of a power function.

Well assessment

Five wells were installed in a line from the upland area to the floodplain, perpendicular to the stream (P0 point, Fig. 1c). The positions were α (upland), the upland-slope border (β), 15 m from the border on the slope (γ), and 30 (δ) and 45 m (ε) from the same border, corresponding to the floodplain. The ε wells were adjacent to the stream. Wells were cased with 7.5 cm-diameter PVC tubes, and were screened with 2 mm openings. The screened sections were covered by a thin fabric (openings 200 μm) to prevent blockage by incoming sediment. The boreholes were then sealed with a mixture of gravel and sand. Finally, the top 25 cm were sealed with swelling bentonite mixed with soil.

The groundwater level was studied by placing HOBO U20-001-01 pressure loggers inside the five monitoring wells; these were the only loggers available in 2015. A small hole was perforated on the sidewall of each PVC well, to equalize internal and external barometric pressures, which is necessary for true barometric compensation. The interval of measurement was also 15 min.

Stream stage variation along the stream

A more detailed survey was undertaken between December 2016 and March 2017, when four additional loggers were placed 622 (P1), 1759 (P2), 2608 (P3) and 2639 m (P4) upstream of P0, following the main reach. Two of these loggers were located in the swamp forest, at about the same altitude, while the two farthest points were 40 m a.s.l. in the mountainous forest, where two tributaries converged to form part of the main reach (Fig. 1b). Thus, P3 and P4 belonged to the sequence P0- P1- P2- P3 (or P4), but the latter two did not form part of the same drainage area.

Due to the availability of equipment, a Levelogger Junior sensor (model 3001, Solinst, Ontario, Canada) had to be used in P1, while in the other stations we employed HOBO dataloggers. All time is referred to in UTC minus 5 hours, according to the time zone where Chile is located (meridian 71° W).

Sensor accuracy

According to the manufacturer, the HOBO logger's operation range is 0 to 207 kPa (approx. 0–9 m water depth at sea level), and from –20 to 50 °C. The typically reported error is 0.5 cm for water level and 0.37°C (at 20°C) for temperature, with a resolution of < 0.02 kPa (0.21 cm water) and 0.1°C (at 20°C) (Onset Computer Corporation, 2005, 2006). Cuevas et al. (2010) experimentally determined that the error for the model used in this study is equivalent to 0.4 cm. On the other hand, the corresponding values for the Levelogger consist of a 10 m range, 0.9 cm error, and 0.27 cm resolution (Solinst, 2011).

Tree evapotranspiration

To investigate one of the possible drivers of the diurnal streamflow pattern, the following species were studied: *Blepharocalyx cruckshanksii*, the most common tree in the swamp forest adjacent to the P1 site (March 24th, 2017); *Eucalyptus nitens*, a common exotic species planted in this area and in southern Chile in general; and *Nothofagus dombeyi*, which is representative of the mountain forest. The two latter species were studied close to the P3 site (March 29th, 2017; Fig. 1b). Three to five healthy leaves were randomly selected from a height of about 1.7 m above the ground from 2–5 individuals per species. We measured the transpiration rate using an Infrared Gas Analyzer (model ADC-LCA4, Analytical Development Co., Hoddesdon, UK). This variable was measured 10-15 times throughout the day, with a phase difference of 10 min from tree to tree. The time lapse was from 7:30 to 17:20 h (UTC–5), given that evapotranspiration is expected to be negligible during night hours (Puchi, 2013). The results were expressed on a leaf area basis and per unit of time, determined by the size of the measurement chamber.

Meteorological variables

A longer meteorological record was obtained for precipitation, air temperature and solar radiation, which were measured every 30 min using a Davis Vantage Pro 2 weather station (Hayward, CA, USA), installed 6 km from the study site in the city of Valdivia (Miraflores; https://centroccbb.cl). Valdivia's potential evapotranspiration (Et_0) was estimated according to the Penman-Monteith equation at an hourly resolution. Relative air humidity was obtained hourly from the Las Lomas (Máfil) station (Campbell Scientific CR 1000, Logan, UT, USA, available from http://agromet.inia.cl), 30 km from the study site, since the other station was unequipped to measure this variable.

Data analyses

Times for maximum and minimum values of the variables of interest were calculated through macros designed with Excel ® software (Microsoft Corporation, Redmond, WA, USA). Times were reported only for those days when the DSS was present. For comparisons of diurnal cycles along the stream we only selected those days that met the following criteria: i) DSS was perceptible through visual inspection of the datalogger records; ii) the amplitude of the signal for both the rising and falling limb of the diurnal hydrogram was above the instrumental error; iii) no rainfall above 1.8 mm fell that day, since this was the threshold that was unable to hide or distort the diurnal signal.

RESULTS

Signal detection

The stream showed clear diurnal fluctuations in water stage, where maximum levels were observed around midday and minimum levels close to midnight (Fig. 2a). The forested slope's groundwater also demonstrated a diurnal fluctuation, although it was slightly more buffered at the rising limb (5 mm) than the stream stage (10 mm), but the converse was observed at the falling limb (19 mm on the slope vs. 11 mm in the stream) (Fig. 2a). Since the stage diminutions were more marked for groundwater, this explains why the stream level was more stable during the analyzed period. Contrary to the aforementioned trends, neither the floodplain (Fig. 2a) nor the upland groundwater (data not shown) showed a discernible diurnal fluctuation.

Visual characterization of the pattern

The visual inspection on January 28th and 29th 2015 revealed that stream level did not fluctuate between 7:30 and 15:30, but did decrease from then onwards (Fig. 3). The minimum level was reached at 1:30 a.m., equivalent to 1 cm less than at the beginning of the inspection. Stream stage recovered 7 mm by 11:00 h, showing lower levels later on. The maximum on January 29th could not be precisely determined because hourly observations were not conducted as they were on the previous day. However, with the help of data logger records it could be determined that this curve followed approximately the direct inspection curve (with the exception of the morning and early afternoon of January 28th). The data logger record peaked between 13:00 and 14:15 on January 29th. The noise in this curve may be associated with instrumental error (0.5 cm) and the disturbance of water flow caused by submerged and emergent woody stems. Observations on February 10th and 11th 2016 showed a smooth pattern, with a minimum level at 7:30 a.m., and a maximum level between 11:30 and 13:30 on February

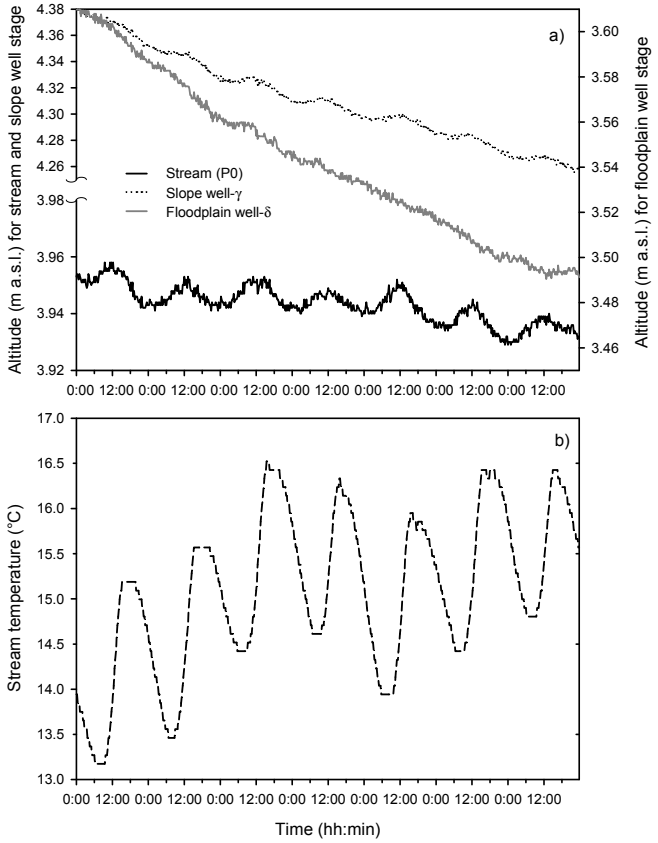

Fig. 2. a) Diurnal stream level variation for a representative week beginning on January 15th 2015. The slope and floodplain groundwater table altitudes are also shown. Ground level is 9.13 m a.s.l. for the slope and 4.83 m for the floodplain. b) Diurnal stream temperature variation for the same week. The upland groundwater (α, β wells) did not show a discernible diurnal level fluctuation and thus data are not shown.

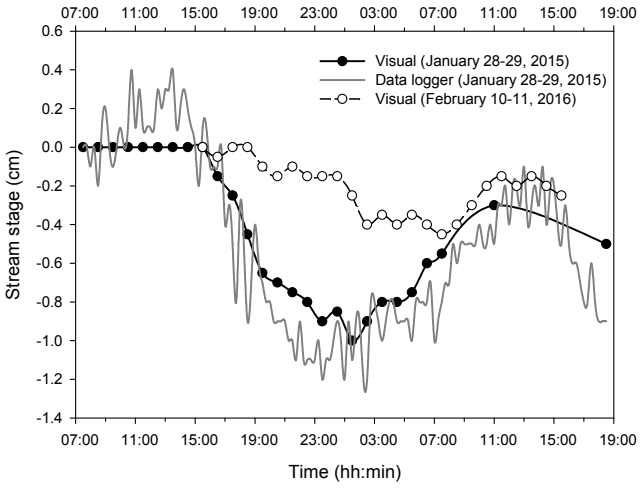

Fig. 3. Diurnal stream stage variation for two dates through visual inspection, contrasted with the data logger record. The water level at the start of the measurements was arbitrarily considered as 0.

11th (Fig. 3). No datalogger records were available for these dates. Generally, the maximum of any given day is lower than the maximum of the previous day. In other words, the decreasing stage trend throughout the night cannot be compensated for by an equivalent rise the next day.

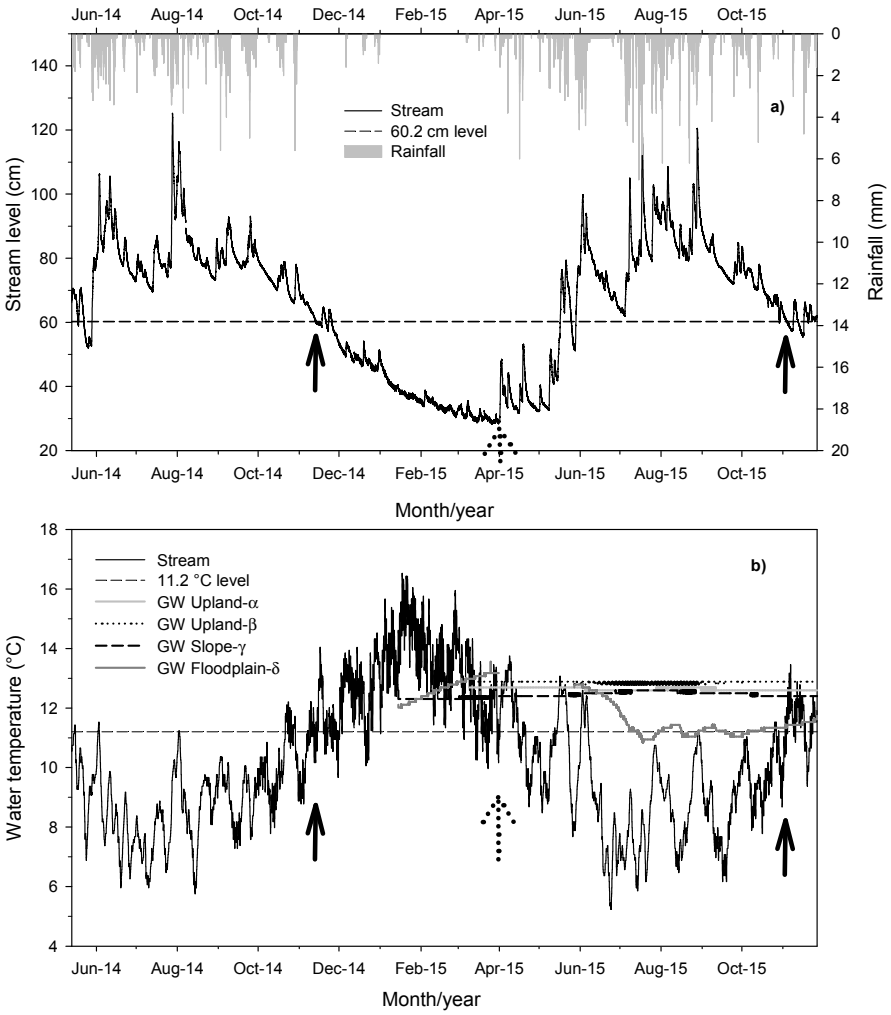

Fig. 4. Temporal fluctuations in stream water level (a), and stream and groundwater (GW) temperature (b). The black arrows indicate the start of the diurnal fluctuation in stream level, while the dotted arrow is the end. The reference lines indicate the values for the appearance or disappearance of this signal.

Signal onset and extinction

The stream level demonstrated large fluctuations throughout the autumn, winter and beginning of spring, due to rainfall events (Fig. 4a). The DSS was first detected on November 14th, 2014 when the stream water stage was 59.6 cm above the streambed. This date corresponds to mid-spring in the Southern Hemisphere, when the growing season is well advanced. The signal remained while the streamflow decreased, even though some sporadic rain events hid the diurnal variation. The signal disappeared on April 1st, 2015 (autumn) when the stream level was 29.2 cm, due to a rain event of 30 mm in 29 hours. No evident signal was detected from April until the beginning of November 2015 (the 3rd day). This time, the stream water stage was 60.9 cm. In general, the DSS was present throughout most of the spring and summer, with a slight trend to decrease in amplitude throughout the season (Fig. 5).

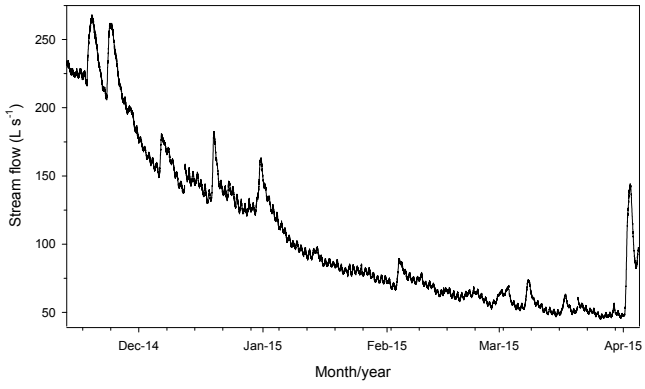

Fig. 5. Seasonal dynamics of the diurnal streamflow variation.

Ground- and surface water temperature

When the DSS appeared in November 2014, the stream temperature was 11.3°C (Fig. 4b). The signal disappeared on April 1st when it was 11.1°C. In the following months, the stream temperature only sporadically surpassed this value. When the signal reappeared on November 3rd, 2015 it was 11.0°C.

Stream temperature experienced repetitive fluctuations throughout the duration of the DSS, from 1.5–2°C each day (Figs. 2b, 4b). These fluctuations are shown in Fig. 4b as more intense and frequent than those corresponding to the rainy season, when the daily temperature fluctuations are not so regular.

Groundwater experienced no temperature fluctuations in upland-α (12.6°C), upland-β (12.9°C), and slope-γ (12.4°C) (Fig. 4b).

Conversely, floodplain-δ groundwater fluctuated between 10.8 and 13.6°C during the first seven months of 2015, and then remained fairly stable towards the end of this year. A diurnal cycle was not detected in any of the studied groundwater.

Signal timing

In November 2014, the maximum stream stage was recorded at 11:00 a.m., on average, with a range covering the entire morning and early afternoon (Table 1). Throughout the season, the maximum water stage became further delayed, reaching 13:00 in March 2015. The minimum water stages were registered late at night, with a progressive temporal shift as the summer season advanced (Table 1).

From January to March, the time of the recorded maximum levels for the forested slope's groundwater varied from 11:42 to 13:22 on average, while the time of the minimum levels ranged from 4:07 to 6:12 (Table 1). The time at which the maximum slope's groundwater table was recorded did not greatly differ from that of the maximum streamflow; however, the time at which the minimum slope's groundwater table was recorded showed a clear delay compared to minimum streamflow.

Stream stage variation along the stream

The P4 station showed stream stage diurnal cycles that, on average, peaked at 6:14 h in the summer (Table 2). P2 reached its maximum at 8:08 h, while the two downstream stations showed maximum stream levels about midday, supporting the previous year's findings for P0. On the other hand, P3, which is located in a different tributary than P4, but which both drain into the Santa Rosa Creek, was rather atypical because its maximum stream stage occurred at 9:25 h (see Discussion). Thus, there was a lag of about 6 h between the highest and lowest stations.

Regarding the minima, the pattern was less distinct than in the previous analysis because P4 showed the lowest stream stages at 19:39 h (summer average), which was very similar to P3 (Table 2). P2, on the other hand, reached the lowest stream levels at 17:27 h, and finally P1 and P0 at 23:39 and 23:48, respectively. When considering all of the studied cases, a lag of 4 h was found between the opposite extremes of the studied stream segment.

Fig. 6 shows the hydrograms for three representative days in the middle of the 2017 summer. For example, on February 2nd P0 was the last to reach its maximum stage at 13:45 h, while P4 was the first at 7:00 h, followed by P3 at 10:45 h, P2 at 11:45 h, and then P1 at 12:30 h.

Once again, the times for the lowest stages had a lower discriminating power for these cycles (Fig. 6). From P4 to P0, the sequence was 20:15, 18:15, 15:45, 20:15, and 20:00–20:15 (P0). For the other days, in general the trend found at the highland stations anticipated that of the lowland sites, for both the maxima and the minima.

Table 1. Time for minimum and maximum stream and slope groundwater stage.

	P2											
Month/year	Stream level maxima			Stream level minima			Slope groundwater maxima			Slope groundwater minima		
	Mean	Min	Max	Mean	Min	Max	Mean	Min	Max	Mean	Min	Max
Nov-2014	11:00	8:30	14:30	0:09	20:45	3:30	nd[a]	nd	nd	nd	nd	nd
Dec-2014	10:55	6:30	13:30	0:34	22:00	4:00	nd	nd	nd	nd	nd	nd
Jan-2015	12:09	9:00	15:00	1:52	23:00	6:00	11:42	9:30	14:30	4:07	0:45	7:15
Feb-2015	12:51	10:45	15:15	1:53	19:45	7:15	12:17	9:00	15:30	3:39	22:15	11:45
Mar-2015	12:59	10:00	15:15	2:28	18:45	7:00	13:22	10:15	15:15	6:12	21:00	11:15

[a]nd: no data since the sensor was installed on site in January 2015.

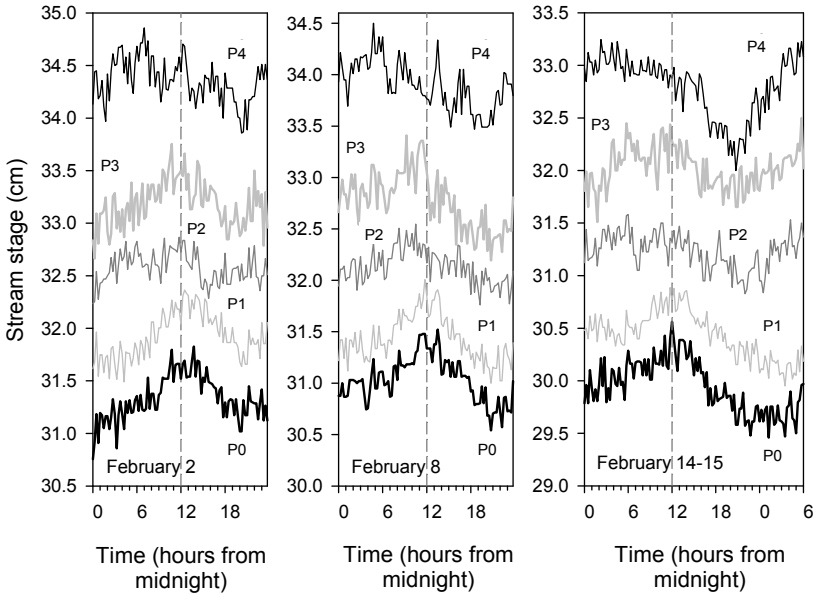

Fig. 6. Variations of stream stage at different stations located in the Santa Rosa Creek, at 0 m (P0, lowest curve), 622 m (P1), 1759 m (P2), 2608 m (P3), and 2639 m (P4, highest curve), upstream of P0. Stage offsets were applied to each curve to decrease the vertical separation among curves, allowing for a simplified comparison of cycles. The vertical dashed line represents midday.

Table 2. Times for maximum and minimum stream stages for points located along the Santa Rosa Creek, at 0 m (P0), 622 m (P1), 1759 m (P2), 2608 m (P3), and 2639 m (P4), upstream of P0. N = sample size for the period December 14th, 2016 to March 9th, 2017.

Station	Time for maximum stream stage				Time for minimum stream stage			
	Mean	Min	Max	N	Mean	Min	Max	N
P0	11:51	7:15	14:45	37	23:48	17:15	9:00	39
P1	12:06	8:45	14:45	12	23:39	19:30	7:30	25
P2	08:08	3:00	14:15	29	17:27	12:30	0:00	27
P3	9:25	3:45	15:30	50	19:23	9:45	23:45	54
P4	6:14	2:15	10:30	26	19:39	14:45	23:00	28

Tree evapotranspiration

Blepharocalyx cruckshanksii showed transpiration rates of 30–750 μmol H_2O m^{-2} s^{-1}, depending on the individual tested and the time of day (Fig. 7a). Maximum values were observed during the morning (8:00 a.m.), while the lowest values were observed at midday. The Et intensified towards the last time analyzed (16:20 h).

On the other hand, *Eucalyptus nitens* (Fig. 7b) showed a clear pattern, where maximum Et occurred around midday, while lower values were observed at earlier and later hours. However, Fig. 7b suggests that there is a secondary peak at 8:00 a.m. Finally, *Nothofagus dombeyi* exhibited a pattern that may be considered a mixture of the other two species' behaviors (Fig. 7c). Et was very high in the early morning (> 2 mmol H_2O m^{-2} s^{-1}), followed by a decrease, and then a recovery after midday. However, Et started to decrease again in the afternoon. Interestingly, the Et experienced diminutions in the middle of the high Et period for both *Eucalyptus* and *Nothofagus*.

Meteorological variables

Fig. 8a shows that air temperature was the highest during the first hours of the afternoon, with its lowest values around 6:00 a.m. The solar radiation cycle anticipated that of the air temperature, which reached its maximum values close to midday, and minimal values (0 W m^{-2}) from 18:00 to 6:00 h, at the end of March 2015 (Fig. 8a). The relative humidity reached values close to 100% even in the summer, peaking before dawn and dropping to its lowest values during the first hours of the afternoon (Fig. 8b). However, since this variable was measured 30 km from our study site, we cannot be sure that the relative humidity was the same in both sites. Potential evapotranspiration (Et_0) also reached its maximum values close to midday, while its minimum or null values were estimated at night (Fig. 8b).

These variables demonstrated no special change in their patterns before the beginning of the DSS in November 2014; their magnitudes simply increased or decreased progressively with the advance of the season (data not shown).

Conversely, at the end of the DSS, April 1st and 2nd, rain profoundly affected all of these variables (Fig. 8). This is apparent when the buffered fluctuations are compared to the period when the DSS was active.

Regarding maximum air temperature, little seasonal temporal shifting was observed (the timing was about 13:00 h, Table 3). Minimum temperatures were registered between 4:07 and 5:14 a.m., on average, when the season progressed.

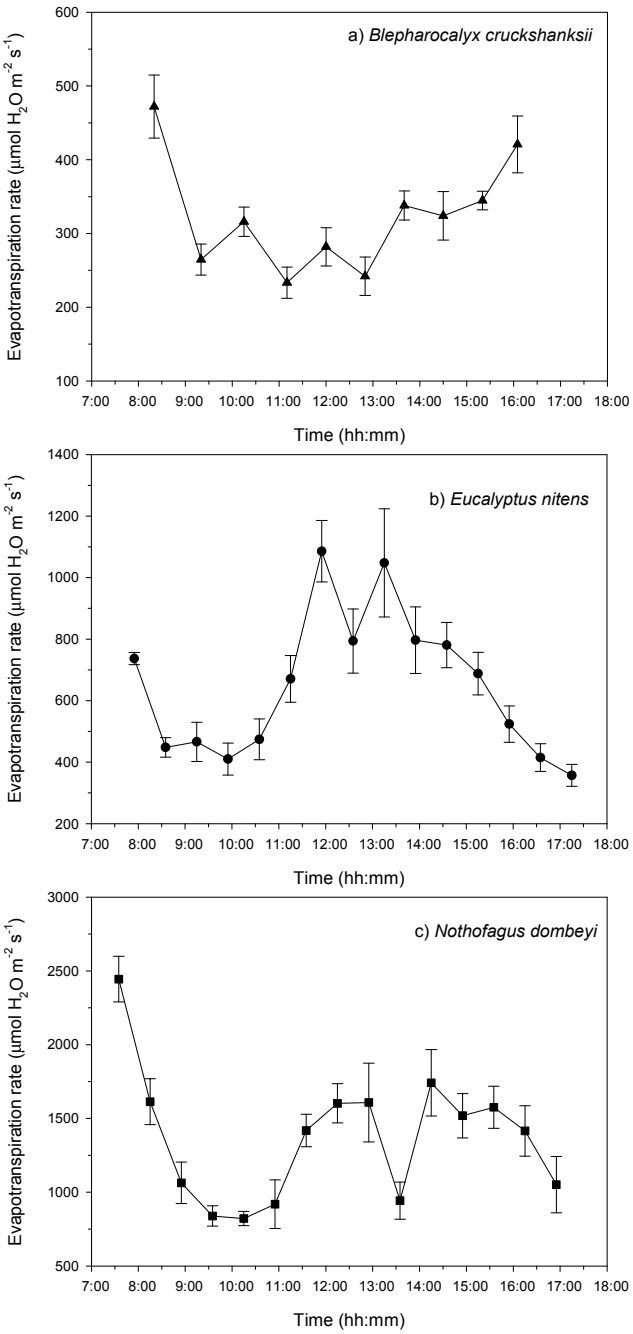

Fig. 7. Evapotranspiration rates for the trees *Blepharocalyx cruckshanksii* (site P1), *Eucalyptus nitens* and *Nothofagus dombeyi* (both at the site P3) throughout the daylight hours. Values are averages ± standard error of 2–5 trees per species, with 3–5 leaves as replicates per tree and per sampling time.

DISCUSSION

Stream and meteorological variables

The visual inspection of the Santa Rosa Creek revealed that the DSS is real. The amplitude of the signal was small, typically 1.0 cm, but higher than the sensor accuracy. Since the noise of most water sensors available in the market is rarely under 0.5 cm, the DSS pattern poses challenges for the detection of small

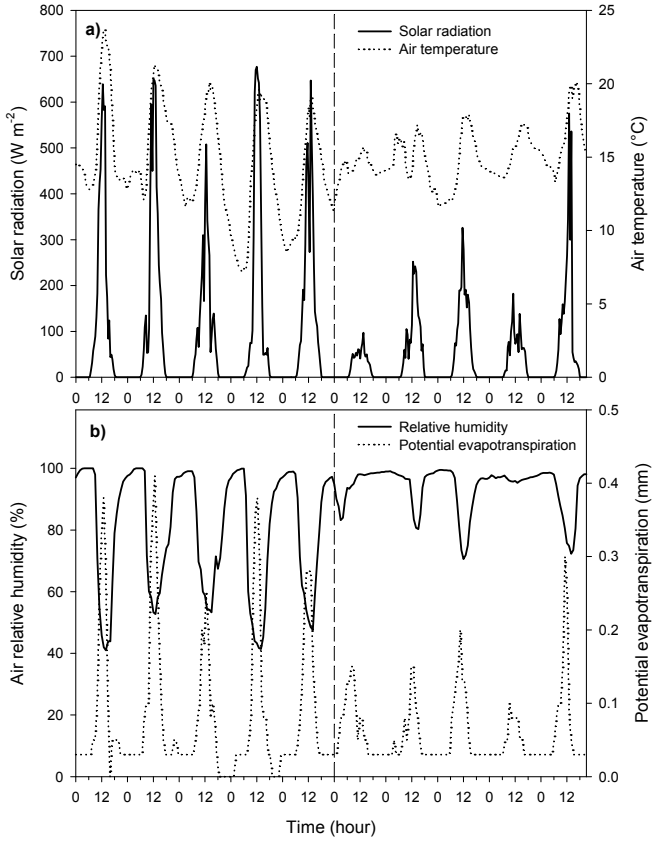

Fig. 8. Variables recorded at the Valdivia (Miraflores) or Máfil (Las Lomas, only relative humidity) meteorological stations at the end of March 2015. a) Air temperature and solar radiation; b) Air relative humidity and potential evapotranspiration. The vertical dashed line corresponds to the end of the diurnal streamflow signal and to the start of the sustained rain (April 1st).

Table 3. Time for minimum and maximum air temperature.

Month/year	Air temperature maxima			Air temperature minima		
	Mean	Min	Max	Mean	Min	Max
Nov-2014	nd[a]	nd	nd	nd	nd	nd
Dec-2014	13:06	10:00	16:00	4:07	21:30	5:30
Jan-2015	13:47	10:00	15:30	4:13	21:30	5:30
Feb-2015	nd	nd	nd	nd	nd	nd
Mar-2015	13:17	12:00	16:00	5:14	21:30	7:30

[a]nd: no data because the meteorological station was out of service.

signals. Thus, the most sensitive and accurate dataloggers should be used for this kind of studies. The DSS appearance when a certain stream stage is reached suggests hydraulic control, while the associated stream temperature at the phenomenon's onset is most likely related to a meteorological effect. The former association is consistent with generalizations about an increase in stream-groundwater exchanges when streamflows and stream stage are lowest (Valett et al., 1997; Voltz, 2011; Wroblicky et al., 1998). On the other hand, the regular pattern in stream temperature variation for the duration of the DSS is most likely related to the regular and intense variations in air temperature (Mohseni and Stefan, 1999) typical of sunny days in the summer. This is fundamentally different from other seasons, when stream temperature is more directly driven by the influx of water during storms (sparse curve patterns). The influence of the aforementioned increase in stream-groundwater exchanges on stream temperature was expected to be smaller than that of the air temperature, because groundwater temperature was nearly constant and did not exhibit a diurnal temperature cycle. This pattern also discards recent causes used to explain the present DSS, such as water viscosity fluctuations (Schwab et al., 2016).

The DSS has also been found to begin when monthly Et_0 surpasses monthly rain in November and ends when this pattern reverses (April; Huertas et al., 2016). Meteorological variables such as air temperature, solar radiation, and Et_0 are well known to progressively increase from winter to summer (Cruz and Calderón, 2008; Sánchez, 2016). The upward crossings of certain levels for these variables (in addition to stream temperature) or downward crossing for air relative humidity, and stream stage, seem to be the indicators related to the onset of the DSS. Thus, the DSS becomes visible at a relatively low stream stage, low air relative humidity, in addition to high air and stream temperatures, and high radiation and Et_0, compared to the weeks prior to the appearance of the DSS. This generalization was fairly coherent for the two spring seasons analyzed.

The end of the DSS was also found to be related to several of the analyzed variables, which either increased or decreased almost suddenly and simultaneously, or demonstrated a lower diurnal fluctuation (Fig. 8). The DSS vanished even though the stream stage was within the range that should have demonstrated a DSS, because the stream flow recovery required a sustained rate of rainfall that hid the DSS. Bond et al. (2002) and Graham et al. (2013) have also pointed out that diurnal streamflow signals are interrupted by rain events and cloud-covered days. Overall, most variables continuously rose or declined from spring to summer, with no abrupt changes that could have triggered the DSS.

Moreover, soil moisture has been found to decrease below a certain threshold value at the DSS start, and recover concomitantly to the DSS extinction (data not shown). This background highlights the importance of catchment storage for DSS appearance, which deserves further research.

Evapotranspiration

If Et is the direct cause of the DSS, corresponding time lags with respect to the streamflow response should occur within a few hours, as has already been reported by Constantz (1998), Bond et al. (2002), Szilágyi et al. (2008), among others. However, in our study, the lag between the maximum expected evaporative demand and the lowest streamflow was about 12 h; the lag between the lowest Et_0 and the highest stream level was up to 8 h.

The time difference may not correspond to our expectations because the temporal cycle of Et_0 is not necessarily the same as that of tree Et. In fact, the analyzed species showed main or secondary maximum rates in the morning (before 8:00 a.m.) and in the late afternoon (after 16:00 h for *B. cruckshanksii*). We have no data for earlier and later hours; thus, the exact moment of maxima throughout the 24 h-cycle is unknown. However, it is expected that Et be very low at night, as shown by other research (Puchi, 2013). Moreover, Zúñiga-Feest et al. (2017) found that two of the main species of the studied swamp forest (*L. apiculata* and *M. exsucca*) have higher stomatal conductance (a proxy of the transpiration rate) early in the morning (8:00–9:00 a.m., UTC − 5) as compared to that which occurs in the afternoon. The probable cause is that stomatal conductance in these seedlings is more responsive to changes in air humidity than to light availability during the day. These greenhouse studies also showed that two other riparian species (*D. winteri* and *B. cruckshanksii*) showed no significant variations in relation to this physiological characteristic throughout the course of

the day. The pattern found for *B. cruckshanksii* in the field should generate a lower streamflow during the first morning hours than that expected for a common Et-driven DSS, and viceversa in the case of the Et minima at midday. However, the floodplain groundwater showed no diurnal signal, probably because water is not a limiting resource in this environment, as tree roots are extensively submerged. Furthermore, during the course of slug tests Huertas et al. (2016) observed a very fast recovery of the floodplain's water table, in the order of minutes, compared to slope wells (30 min) and upland wells (more than 1 h). The slope's groundwater could be difficult to relate to the local Et because its diurnal fluctuations were also very out-of-time with respect to common Et-cycles. Thus, the diurnal signal found under the slope-γ could reflect a dragging, delayed effect from the stream, rather than the cause of the DSS.

The signal has been found to vanish under the uplands where grassland roots cannot influence the groundwater table 7–8 m belowground (Cuevas et al., 2014). This is coherent with a study in headwater catchments in Oregon, USA, where Voltz (2011) also found that the amplitude of the diurnal groundwater table variation is maximal at intermediate distances from the stream.

The two species belonging to the mountain forest had Et cycles similar to that expected for typical forest species, with some important diminutions at the peak of the evaporative demand, probably related to the decrease of stomatal conductance that we measured in parallel (data not shown). This indicates that these species can restrict their water loss and do not simply behave as a passive water reservoir. Puchi (2013) also found that *Eucalyptus globulus* has Et cycles with maximum transpiration rates close to midday, with very low values at night.

Interpretation of the diurnal signal

Our results show that the DSS reached maximum values early in the morning for the stations located in the headwater mountain forest areas, coherent with a typical Et control. The maximum appeared progressively later downstream. P3 did not demonstrate the exact same timing as P4. If we consider that they belong to different tributaries, it is not surprising that they have a different DSS. No data is available for explaining this discrepancy, but perhaps some heterogeneity in apparently homogeneous watersheds exists, given the differences in vegetation cover, slopes, aspects, drainage area, etc.

The minimum values of DSS also occurred earlier in the mountainous area, but later than the expected time (19:30 h). Usually, the lowest streamflows occur during the first hours of the afternoon (13:30–16:30 h; Wondzell et al., 2007; Gribovszki et al., 2008; Cuevas et al., 2010). In addition to a delay between maximum Et and the previously reported stream response (Bond et al., 2002; Constantz, 1998; Szilágyi et al., 2008), we must consider that the watershed begins 1.5–2.0 km upstream of our highest monitoring points (P3 and P4), which may explain the relatively late time for the stream minima, if the DSS does indeed originate upstream.

In fact, the present evidence suggests that the DSS is a wave that originates in the mountainous forests and travels through the tributaries that drain to the Santa Rosa Creek. We recorded a short lag between the timing for the observed Et cycles, which would reach their minimum values at night, and the corresponding maximum streamflows. However, when the streamflow enters the swamp forest, we found this vegetation cover (and the adjacent deciduous forest) unable to generate an Et cycle that could impact ground- and surface waters. Thus, the signal appeared to be progressively decoupled from the vegetation cycles. Finally, when the DSS reached P0 it was fully reversed with respect to the expected timing.

The origin of the Et-driven DSS in the mountains located in the headwaters may have to do with the second-growth evergreen forests and exotic tree plantations (less than 20 years old) found there, which are in an active period of growth, with comparatively high Et rates. Exotic *Eucalyptus* trees are especially well known for their high Et (Fetene and Beck, 2004; Scott and Prinsloo, 2008). However, the cover of this species alone (0.74% in the Santa Rosa catchment) may not be the only factor controlling stream levels. Cuevas et al. (2010), working in the Coastal Mountain Range of southern Chile, found a clear DSS. Its watershed had a 69% cover of *Eucalyptus*, but even in those areas covered entirely by native forest the pattern was still clear. Thus, native species also have the potential to influence the stream stage, despite their lower Et rates compared to *Eucalyptus* trees (Jiménez-Castillo et al., 2011; Puchi, 2013).

Moreover, different soil orders may also be involved in the diverse responses of streams to Et cycles. Andisols, which have a large water holding capacity (Dörner et al., 2009), are typical of the swamp forest, while Ultisols dominate the mountain headwaters. Given that Cuevas et al. (2010) also detected a clear DSS on Ultisols, further research should clarify how the different hydraulic properties of these soils modulate the transmission of Et signals towards the stream.

In small headwater catchments, the DSS would most likely propagate very quickly as found by Cuevas et al. (2010), but in those with an important flat zone, such as the studied swamp forest, the time lag could be much longer. Long time lags, such as those found in this study, have scarcely been reported in the literature (Wondzell et al., 2007), and when they were established they were analyzed in a different context than our research. For instance, Voltz (2011) showed that the DSS minimum ranged from 15:00 to 1:00 h, while the DSS maximum varied from 2:00 to 10:00 h, suffering a progressive delay with the advance of the season. Graham et al. (2013) found lags of up to 9 hours between the sap flow and the DSS. These patterns have been explained based on Wondzell et al. (2007), who considered Et to be a signal generated over an entire catchment, where at low flows the reduced stream velocity could (conceptually) produce a destructive interference of down-network traveling signals, masking some or all of the upstream signals. This hypothesis received support from Graham et al. (2013), but in our study the net result was the DSS delay due to the long travel time from the mountains.

Our interpretation of the DSS lag is a little different from Wondzell et al. (2007), Voltz (2011) and Graham et al. (2013) given that their watersheds were relatively homogeneous in their riparian vegetation, soil, and slope along the same stream channel. In our case, these factors change along the altitudinal gradient, and thus highlight the role of landscape heterogeneity in shaping hydrological processes. It would be interesting to determine if the DSS lag still persists in watersheds with old-growth forests in the uplands, vegetation which was never replaced by grasslands.

CONCLUSIONS

The diurnal streamflow pattern examined in this paper shows the complex interrelationship between atmospheric variables (air temperature, solar radiation, air relative humidity), plant cover (Et), geomorphology, land cover, and stream and groundwater stage. Meteorological variables showed no special consistent changes during the onset of the DSS, instead the crossing of environmental values appears to activate this

stream signal. This is most likely caused by intensified evapotranspiration cycles from late spring onwards, when water becomes a limiting resource. Conversely, the end of the signal was profoundly influenced by rain, which strongly affects the meteorological, plant, soil, and water variables. We propose that stream stage delays with respect to a typical Et cycle are due to the great distance between source areas high in the mountains (covered by second-growth evergreen native forests and exotic tree plantations) and the lowland zones covered by swamp forest, under a scenario of null influence of local Et on stream stage. These long lags make the cause-and-effect relationship of local Et and stream stage seem non-apparent or even positively and spuriously related. Diurnal fluctuations in streamflow are more complex than presently considered by accepted models, and we concur with Gribovski et al. (2010) that this topic deserves further study.

Acknowledgements. Funding was provided by Fondecyt grant 1110156. INIA hosted the first author during the phase of data collection. We would like to thank the Santa Rosa Experimental Station staff for their help, especially the Administrator Carlos Villagra. JC also thanks his deceased colleague Miguel Ángel López (INIA Quilamapu) for designing the macro used in this paper Felipe Labra (INFOR) drew the Fig. 1. Logistical support was provided by Mr. César Lemus, Mlle. Mélanie Krauth, and especially Rodrigo Bravo. Dr. José Dörner provided some helpful ideas for earlier versions of this paper. Additional acknowledgements go to Dr. Carlos Oyarzún (Universidad Austral de Chile), who supported this research, Dr. Antonio Lara and Mr. David Lobos from CR^2 (Center for Climate and Resilience Research) for lending us part of the equipment used in this study, and to the Water Center CRHIAM Conicyt/Fondap/15130015 for supporting part of the data analysis and the English edition of the document. Finally, two anonymous reviewers contributed with helpful suggestions.

REFERENCES

Amigo, J., Ramírez, C., 1998. A bioclimatic classification of Chile: woodland communities in the temperate zone. Plant Ecol., 136, 1, 9–26.

Barnard, H., Graham, C., Van Verseveld, W., Brooks, J., Bond, B., McDonnell, J., 2010. Mechanistic assessment of hillslope transpiration control of diel subsurface flow: a steady-state irrigation approach. Ecohydrology, 3, 2, 133–142.

Bond, B.J., Jones, J.A., Moore, G., Phillips, N., Post, D., McDonnell, J.J., 2002. The zone of vegetation influence on baseflow revealed by diurnal patterns of streamflow and vegetation water use in a headwater basin. Hydrol. Process., 16, 8, 1671–1677.

Bren, L.J., 1997. Effects of slope vegetation removal on the diurnal variation of a small mountain stream. Water Resour. Res., 33, 2, 321–331.

Brooks, J., Barnard, H., Coulombe, R., McDonnell, J., 2010. Ecohydrologic separation of water between trees and streams in Mediterranean climate. Nat. Geosci., 3, 2, 100–104.

Burt, T.P., 1979. Diurnal variations in stream discharge and throughflow during a period of low flow. J. Hydrol., 41, 3–4, 291–301.

Caine, N., 1992. Modulation of the diurnal streamflow response by the seasonal snowcover of an alpine basin. J. Hydrol., 137, 1, 245–260.

Carlson Mazur, M.L., Wiley, M.J., Wilcox, D.A., 2014. Estimating evapotranspiration and groundwater flow from water-table fluctuations for a general wetland scenario. Ecohydrology, 7, 2, 378–390. DOI:10.1002/eco.1356.

CIREN (Centro de Información de Recursos Naturales), 2001. Estudio Agrológico X Región, Tomo I. CIREN, Santiago, Chile.

Constantz, J., 1998. Interaction between stream temperature, streamflow, and groundwater exchanges in alpine streams. Water Resour. Res., 34, 7, 1609–1615.

Cruz, C., Calderón, J., 2008. Guía climática práctica. [online] Dirección Meteorológica de Chile, p.117. Available at: http://164.77.222.61/climatologia/publicaciones/climatica_practica.pdf [Accessed 26 Jul. 2016].

Cuevas, J.G., Calvo, M., Little, C., Pino, M., Dassori, P., 2010. Are diurnal fluctuations in streamflow real? J. Hydrol. Hydromech., 58, 3, 149–162.

Cuevas, J.G., Huertas, J., Leiva, C., Paulino, L., Dörner, J., Arumí, J.L., 2014. Nutrient retention in a microwatershed with low levels of anthropogenic pollution. Bosque, 35, 1, 75–88.

Dörner, J., Dec, D., Peng, X., Horn, R., 2009. Change of shrinkage behavior of an Andisol in southern Chile: Effects of land use and wetting/drying cycles. Soil Till. Res., 106, 1, 45–53.

Dörner, J., Dec, D., Peng, X., Horn, R., 2010. Effect of land use change on the dynamic behaviour of structural properties of an Andisol in southern Chile under saturated and unsaturated hydraulic conditions. Geoderma 159, 1–2, 189–197.

Fetene, M., Beck, E., 2004. Water relations of indigenous versus exotic trees species, growing at the same site in a tropical montane forest in southern Ethiopia. Trees, 18, 4, 428–435.

Graham, C.B., Barnard, H.R., Kavanagh, K.L., McNamara, J.P., 2013. Catchment scale controls the temporal connection of transpiration and diel fluctuations in streamflow. Hydrol. Process., 27, 18, 2541–2556.

Gribovszki, Z., Kalicz, P., Szilágyi, J., Kucsara, M., 2008. Riparian zone evapotranspiration from diurnal groundwater level fluctuations. J. Hydrol., 349, 1, 6–17.

Gribovszki, Z., Szilágyi, J., Kalicz, P., 2010. Diurnal fluctuations in shallow groundwater levels and streamflow rates and their interpretation – A review. J. Hydrol., 385, 1–4, 371–383.

Gribovszki, Z., Kalicz, P., Szilágyi, J., 2013. Does the accuracy of fine-scale water level measurements by vented pressure transducers permit for diurnal evapotranspiration estimation? J. Hydrol., 488, 166–169.

Huertas, J., Cuevas, J.G., Paulino, L., Salazar, F., Arumí, J.L., Dörner, J., 2016. Dairy slurry application to grasslands and groundwater quality in a volcanic soil. J. Soil Sci. Plant Nutrit., 16, 3, 745–762.

Hughes, D.A., 2010. Unsaturated zone fracture flow contributions to stream flow: evidence for the process in South Africa and its importance. Hydrol. Process., 24, 6, 767–774.

Jiménez-Castillo, M., Lobos-Catalán, P., Aguilera-Betti, I., Rivera, R., 2011. Daily transpiration rates and hydraulic relationships in tree species with different shade-tolerance level in a Chilean temperate forest. Gayana Bot., 68, 2, 155–162. (In Spanish.)

Jordon, P., 1983. Meltwater movement in a deep snowpack. 1. Field observations. Water Resour. Res., 19, 4, 971–978.

McLaughlin, D.L., Cohen, M.J., 2011. Thermal artifacts in measurements of fine-scale water level variation. Water Resour. Res., 47, W09601.

Mohseni, O., Stefan, H.G., 1999. Stream temperature/air temperature relationship: a physical interpretation. J. Hydrol., 218, 3–4, 128–141.

Moore, G., Jones, J., Bond, B.J., 2011. How soil moisture mediates the influence of transpiration on streamflow at hourly

to interannual scales in a forested catchment. Hydrol. Process., 25, 24, 3701–3710.

Mutzner, R., Weijs, S.V., Tarolli, P., Calaf, M., Oldroyd, H.J., Parlange, M.B., 2015. Controls on the diurnal streamflow cycles in two subbasins of an alpine headwater catchment. Water Resour. Res., 51, 5, 3403–3418. DOI: 10.1002/2014WR016581.

Onset Computer Corporation, 2005, 2006. HOBO® U20 Water Level Logger (Part # U20-001-01). Doc # 8976-G, MAN-U20-001-01. Bourne, Massachusetts, USA.

Puchi, P.F., 2013. Influencia de la transpiración sobre la variación del caudal a escala horaria en una microcuenca cubierta con *Eucalyptus globulus* Labill. Master thesis, Faculty of Sciences, Universidad Austral de Chile, Valdivia, Chile. 56 p + xiv.

Sánchez, S., 2016. Comportamiento de la radiación ultravioleta (UV-B) en Chile. Dirección Meteorológica de Chile. Available at: http://164.77.222.61/climatologia/publicaciones/Comportamiento_radiacion_UV-B.pdf [Accessed 26 Jul. 2016].

Schwab, M., Klaus, J., Pfister, L., Weiler, M., 2016. Diel discharge cycles explained through viscosity fluctuations in riparian inflow. Water Resour. Res., 52, 11, 8744–8755. DOI: 10.1002/2016WR018626.

Scott, D., Prinsloo, F., 2008. Longer-term effects of pine and eucalypt plantations on streamflow. Water Resour. Res., 44, 7, W00A08.

Soil Survey Staff, 1999. Soil taxonomy: A basic system of soil classification for making and interpreting soil surveys. 2nd Ed. Natural Resources Conservation Service, U.S. Department of Agriculture Handbook 436, Washington D.C., USA.

Solinst, 2011. User Guide Levelogger Series Software Version 4. Solinst Canada Ltd., 35 Todd Road, Georgetown, ON, L7G 4R8st Canada.

Szilágyi, J., Gribovszki, Z., Kalicz, P., Kucsara, M., 2008. On diurnal riparian zone groundwater-level and streamflow fluctuations. J. Hydrol., 349, 1–2, 1–5.

Valett, H.C., Dahm, C.N., Campana, M.E., Morrice, J.A., Baker, M.A., Fellows, C.S., 1997. Hydrologic influences on groundwater-surface water ecotones: heterogeneity in nutrient composition and retention. J. N. Am. Benthol. Soc., 16, 1, 239–247.

Voltz, T.J., 2011. Riparian hydraulic gradient and water table dynamics in two steep headwater streams. Thesis in Ms Civil Engineering. The Pennsylvania State University, USA, 150 p.

Wain, A.S., 1994. Diurnal river flow variations and development planning in the tropics. Geogr. J., 160, 3, 295–306.

Wondzell, S.M., Gooseff, M.N., McGlynn, B.L., 2007. Flow velocity and the hydrologic behavior of streams during baseflow. Geophysical Research Letters 34, L24404. DOI: 10.1029/2007GL031256.

WRB (World Reference Base for Soil Resources), 2006. World reference base for soil resources. A framework for international classification, correlation and communication. 2nd Ed. FAO, World Soil Resources Reports No. 103, Rome, Italy.

Wroblicky, G.J., Campana, M.E., Valett, H.M., Dahm, C.N., 1998. Seasonal variation in surface-subsurface water exchange and lateral hyporheic area of two stream-aquifer systems. Water Resour. Res., 34, 3, 317–328.

Zúñiga-Feest, A., Bustos-Salazar, A., Alves, F., Martínez, V., Smith-Ramírez, C., 2017. Physiological and morphological responses to permanent and intermittent waterlogging in seedlings of four evergreen trees of temperate swamp forests. Tree Physiol., 37, 6, 776–789. DOI: 10.1093/treephys/tpx023.

Received 2 May 2017
Accepted 24 July 2017